Acta Pharmacologica Sinica (2013) 34: 1140–1148
 1671-4083/13 $32.00
www.nature.com/aps

Original Article

Quercetin protects rat dorsal root ganglion neurons against high glucose-induced injury *in vitro* through Nrf-2/HO-1 activation and NF-κB inhibition

Yue SHI[1], Xiao-chun LIANG[1, *], Hong ZHANG[2], Qun-li WU[1], Ling QU[1], Qing SUN[1]

[1]Department of Traditional Chinese Medicine, Peking Union Medical College Hospital, Chinese Academy of Medical Sciences and Peking Union Medical College, Beijing 100730, China; [2]Department of Pathology, Institute of Basic Medical Sciences, Chinese Academy of Medical Sciences, School of Basic Medicine, Peking Union Medical College, Beijing 100005, China

Aim: To examine the effects of quercetin, a natural antioxidant, on high glucose (HG)-induced apoptosis of cultured dorsal root ganglion (DRG) neurons of rats.
Methods: DRG neurons exposed to HG (45 mmol/L) for 24 h were employed as an *in vitro* model of diabetic neuropathy. Cell viability, reactive oxygen species (ROS) level and apoptosis were determined. The expression of NF-κB, IκBα, phosphorylated IκBα and Nrf2 was examined using RT PCR and Western blot assay. The expression of hemeoxygenase-1 (HO-1), IL-6, TNF-α, iNOS, COX-2, and caspase-3 were also examined.
Results: HG treatment markedly increased DRG neuron apoptosis via increasing intracellular ROS level and activating the NF-κB signaling pathway. Co-treatment with quercetin (2.5, 5, and 10 mmol/L) dose-dependently decreased HG-induced caspase-3 activation and apoptosis. Quercetin could directly scavenge ROS and significantly increased the expression of Nrf-2 and HO-1 in DRG neurons. Quercetin also dose-dependently inhibited the NF-κB signaling pathway and suppressed the expression of iNOS, COX-2, and proinflammatory cytokines IL-6 and TNF-α.
Conclusion: Quercetin protects rat DRG neurons against HG-induced injury *in vitro* through Nrf-2/HO-1 activation and NF-κB inhibition, thus may be beneficial for the treatment of diabetic neuropathy.

Keywords: quercetin; antioxidant; diabetic neuropathy; dorsal root ganglion; reactive oxygen species; Nrf-2; hemeoxygenase-1; NF-κB; proinflammatory cytokine

Acta Pharmacologica Sinica (2013) 34: 1140–1148; doi: 10.1038/aps.2013.59; published online 10 June 2013

Introduction

Diabetes is the most common cause of peripheral neuropathy in the world. Most patients with diabetes have neuropathy[1], and the prevalence of neuropathy in patients with prediabetes is rising. Diabetic neuropathy is a major cause of disability and health care costs[2, 3]. Patients with diabetes are prone to peripheral nerve disorders, which may present as pain, numbness, tingling, weakness, and difficulties with balance. Thus far, there is still no approved therapy for treating diabetic neuropathy.

Peripheral neuropathy can be attributed to numerous mechanisms, including sorbitol accumulation, oxidative-nitrosative stress, 12/15-lipoxygenase activation, inflammation, the polyol pathway, and poly (adenosine diphosphate [ADP]-ribose) polymerase (PARP) overactivation[4, 5]. Among these mechanisms, oxidative-nitrosative stress, which interacts with many other pathways implicated in diabetic neuropathy, is often considered to be the most critical[6].

Hyperglycemia can increase levels of reactive oxidative species (ROS) through both enzymatic and nonenzymatic processes. Once absorbed by cells, sugar molecules serve as substrates for cellular respiration pathways (*ie*, glycolysis and the tricarboxylic acid cycle) that produce reducing equivalents that then drive oxidative phosphorylation in mitochondria, a process that produces ROS. Glucose autoxidation creates free radicals that can damage cellular proteins and mitochondrial DNA[7]. Cells possess an array of antioxidant defense machinery to prevent or counterbalance damage caused by reactive radicals. A family of enzymes exists that detoxify highly reactive radicals to protect cells against excessive oxidative stress. Highly toxic metabolites are generated from phase I detoxification reactions and must be detoxified quickly by phase II

* To whom correspondence should be addressed.
E-mail xcliang0704@sina.com
Received 2013-03-01 Accepted 2013-04-12

detoxifying enzymes, such as glutathione S-transferase, UDP glucuronyltransferase, heme oxygenase-1 (HO-1), NADPH-quinone oxidoreductase, and microsomal epoxide hydrolase. A build-up of phase I metabolites can wreak havoc on cells. The transcription factor nuclear factor (erythroid-derived 2)-like 2 (Nrf-2) is recognized as a critical factor in the induction of phase II enzymes[8].

Oxidative stress results in the activation of NF-κB, which triggers the activation of inflammatory signaling pathways[7]. NF-κB is a rapid-acting pleiotropic transcription factor that regulates a diverse group of genes, including genes that encode inducible nitric oxide synthase (iNOS), cyclooxygenase-2 (COX-2), and proinflammatory cytokines. In experimental diabetic neuropathy models, ROS-activated NF-κB and its oxidant products have been shown to enhance the expressions of iNOS, COX-2, tumor necrosis factor-alpha (TNF-α), and interleukin (IL)-6[9–11]. Oxidative stress and inflammation have been shown to interact with each other and to be inseparably linked to diabetic neuropathy.

Treatments that are currently prescribed to lessen neuropathic pain have undesirable secondary effects and situational variable efficacy[12]. Therefore, researchers are searching for better diabetic neuropathy drug options. Flavonoids are an attractive treatment option, given their efficacy in clearing ROS and their ability to protect against neuronal damage[13]. The flavonoid quercetin is the most potent scavenger of ROS, including superoxide, and reactive nitrogen species[14]. Furthermore, quercetin reduces low-density lipoprotein oxidation and suppresses iNOS activity, consequently reducing damage from nitric oxide superoxide anions[15].

The axons of dorsal root ganglion neurons (DRG neurons) are afferents that relay sensory information to the central nervous system. With their exuberant metabolism and sensitivity to high glycemia, DRG neurons are an experimental target of diabetic neuropathy[16, 17]. Even short-term hyperglycemia can produce oxidative damage and apoptosis in DRG neurons[17]. Inflammatory factors play an important role in DRG neuronal damage, especially in painful neuropathy[9, 18, 19]. In previous studies, lower glucose concentrations induced DRG neuron death in culture, whereas total glucose levels above 35 mmol/L produced hyperglycemic insult leading to DRG neuron death[20]. To produce a hyperglycemic insult, 20 mmol/L additional glucose (yielding a total 45 mmol/L glucose) were added to the media for the period specified in individual experiments.

In this study, we evaluated the effects of quercetin (2.5, 5, and 10 mmol/L) on high glucose (HG)-treated DRG neurons, in terms of cell viability, ROS levels, and apoptosis. The expression levels of NF-κB, Nrf2/HO-1, proinflammatory mediators (IL-6 and TNF-α), iNOS, COX-2, and caspase-3 were also evaluated.

Materials and methods

Cell culture and treatments

Unless otherwise noted, cell culture materials and other reagents were obtained from Sigma (St Louis, MO, USA). DRG neurons were harvested from Sprague-Dawley rats (Vital River Company, China) at embryonic d 15. Prior to their establishment in culture, the neurons were digested with 0.25% trypsin in D-Hanks' solution at 37 °C for 20 min. After digestion and dissociation, fetal bovine serum (Invitrogen, Grand Island, NY, USA) was added to a final concentration of 10% to stop digestion. Cells were passed through a 74-μm filter and centrifuged for 5 min at 201.24×*g*. The pellet was resuspended in neurobasal medium (Invitrogen, Grand Island, NY, USA) of 2% B-27 supplement without antioxidants (Invitrogen, Grand Island, NY, USA), 10 ng/mL nerve growth factor (Merck-Millipore, Darmstadt, Germany), 1 mmol/L *L*-glutamine, and 1000 U/mL of penicillin/streptomycin/neomycin (ABX, North China Pharmaceutical Group Corp, Shijiazhuang, China) solution.

Dissociated DRG cells were cultured in poly-D-lysine-precoated 96-well or 6-well clusters (Costar, Corning, NY) at 5×10^4 cells/well in 0.1 mL for 96-well clusters or 2×10^6 cells/well in 2 mL for 6-well clusters. DRG cells were cultured in media at 37 °C with 5% CO_2 and maintained in media containing 20 μmol/L FUDR for another 24 h to inhibit the growth of non-neuronal cells. The purity of neuronal cells was confirmed by fluorescent labeling of microtubule-associated protein 2 (MAP-2, Merck-Millipore) and a 4′,6-diamidino-2-phenylindole (DAPI, Zhongshan Golden Bridge Biotechnology Co, Ltd, Beijing, China) fluorescent counterstain (Figure 1). Neurons were cultured for an additional 24 h under different experimental conditions before examination.

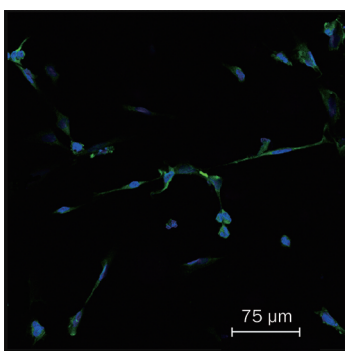

Figure 1. Double fluorescent labeling of MAP-2 and DAPI. MAP-2-labeled DRG neurons, DAPI-labeled nuclei of all cells in culture. (Scale bar=75 μm).

Neurobasal medium was used as the control group medium because its glucose concentration is 25 mmol/L, which is optimal for the survival and growth of DRG neurons. An additional 20 mmol/L glucose was added to the medium for the HG groups[17]. The cells were randomly divided into five groups: control (CON, 25 mmol/L glucose), HG (45 mmol/L glucose), and HG plus 2.5 mmol/L quercetin (Q2.5), 5 mmol/L quercetin (Q5), or 10 mmol/L quercetin (Q10). The choice of quercetin concentrations was based on our unpublished results.

Cell viability assay

DRG neurons were plated into 96-well clusters at a density of 5×10^4 cells/well. After a 24-h incubation under group-specified experimental conditions, the clustered neurons were processed for detection of cell viability by 3-(4,5-dimethyldiazol-2-yl)-2,5-diphenyltetrazolium bromide (MTT) assays. Briefly, 100 μL of 5 mg/mL stock solution of MTT was added to each well and incubated at 37 °C for 4 h, after which 100 μL of dimethyl sulfoxide (DMSO) was added to each well. Absorbance was measured at 570 nm with a microplate reader. Cell viability was expressed as the ratio of clustered neurons to control cells.

Determination of apoptotic cells

After a 24-h incubation (2×10^6 cells/well) on poly-*D*-lysine–coated coverslips in 6-well plates according to group specifications, apoptotic cells were detected by the terminal deoxynucleotidyltransferase-mediated UTP nick end-labeling (TUNEL) method with an in situ cell death detection kit (Roche, Mannheim, Germany), according to the manufacturers' instructions. After detection by fluorescence microscopy at an excitation wave length of 530 nm, the cells were added to a converter-POD, stained with diaminobenzidine (DAB, Zhongshan Golden Bridge Biotechnology Co, Ltd, Beijing, China), counterstained with hematoxylin, and examined by light microscopy. Cells treated with DNase I (Fermentas, Burlington, Canada) were used as positive controls. Cells labeled with the reaction mixture, but without terminaltransferase, were used as negative controls. Apoptotic cells were examined under a light microscope; at least 500 cells from each group were examined in a blinded manner.

Measurement of ROS

Intracellular ROS was measured with the cell-permeable oxidation-sensitive fluorescent probe 2′,7′-dichlorofluorescein diacetate (DCFH-DA, Molecular Probes, and Eugene, OR). DCFH-DA freely diffuses into cells, where it is cleaved into DCFH by intracellular esterase, which cannot pass out of the cell. In the presence of ROS, DCFH becomes oxidized into a fluorescent product, DCF, which serves as an index to indicate intracellular ROS levels. DCFH-DA was dissolved freshly in neurobasal medium and used at a final concentration of 5 μmol/L.

Based on our preliminary results, ROS in the HG group were elevated from 1 h, peaked at 4 h, and thereafter declined; therefore, 4 h was chosen as the time point for analysis. After 4 h of HG treatment, cells were harvested and treated with 5 μmol/L DCFH-DA at 37 °C for 30 min in the dark. After DCFH-DA treatment, the culture medium was removed, and the cells were washed with 0.1 mmol/L phosphate-buffered saline (PBS, pH 7.4, Invitrogen) three times to remove excess probe. Fluorescence intensity was analyzed by flow cytometry with histogram plots. ROS values were calculated relative to unlabeled control cells.

Quantitative real-time reverse transcription polymerase chain reaction (qRT-PCR)

Total RNA was extracted with the TRIzol® RNA isolation reagent (Invitrogen). Reverse transcription was performed with a PrimeScript® RT Master Mix kit (TAKARA Biotechnology Co, Ltd, Dalian). The cDNA products were subjected to real-time PCR with the SYBR premixed system and specific primers. Real-time PCR was performed in a StepOnePlus™ Real-Time PCR System (Applied Biosystems) by using the following program: 95 °C for 10 min, followed by 40 cycles of 95 °C for 15 s, and 60 °C for 1 min. Each sample was analyzed in triplicate. β-actin mRNA was quantified in each sample as an endogenous control. The sequences of the primers used are summarized in Table 1. Nucleotide BLAST and melting curve analyses were used to confirm primers specificity.

Table 1. Primer and probe sequences.

Protein	Reference	Direction	Sequence
Nrf-2	21	Sense	5′-GCAACTCCAGAAGGAACAGG-3′
		Antisense	5′-GGAATGTCTCTGCCAAAAGC-3′
HO-1	22	Sense	5′-CTTTCAGAAGGGTCAGGTGTC-3′
		Antisense	5′-TGCTTGTTTCGCTCTATCTCC-3′
NF-κB	23	Sense	5′-CATGCGTTTCCGTTACAAGTGCGA-3′
		Antisense	5′-TGGGTGCGTCTTAGTGGTATCTGT-3′
IL-6	24	Sense	5′-CAGGGAGATCTTGGAAATGA-3′
		Antisense	5′-AACTCCAGAAGACCAGAGCA-3′
TNF-α	25	Sense	5′-TACTGAACTTCGGGGTGATTG-3′
		Antisense	5′-CAGCCTTGTCCCTTGAAGAGA-3′
iNOS	26	Sense	5′-TGAACTTGAGCGACGGACCA-3′
		Antisense	5′-TTCATGTGATAACGTTTCTGGCTCT-3′
COX-2	27	Sense	5′-TGATCGAAGACTACG TGCAACAC-3′
		Antisense	5′-CAGCAATCTGTCTGGTGAATGAC-3′
Caspase-3	28	Sense	5′-GCCGAAACTCTTCATCATTCAGG-3′
		Antisense	5′-CATATCATCGTCAGTTCCACTGTC-3′

Western blot analysis

Total protein was isolated with protein lysis buffer supplemented with phenylmethanesulfonyl fluoride (Beyotime Institution of Biotechnology, Haimen, China) and protease inhibitor (AmrescoLLC, Solon, OH, USA). Protein samples were separated by 10% SDS-PAGE (Beyotime Institution of Biotechnology) and transferred to NC membranes (Pall Gelman Laboratory, Ann Arbor, MI, USA). Subsequently, the membranes were blocked with 5% fat-free milk and incubated with primary antibodies against iNOS, COX-2, NF-κB (p65), IκBα, phospho IκBα, and β-actin (Santa Cruz Biotechnology, Santa Cruz, CA, USA), Nrf-2, HO-1, and caspase-3. All Santa Cruz antibodies were used at a dilution of 1:200. Anti-NRf-2 was used at 1:500, and anti-HO-1 and anti-caspase-3 were used at 1:1000.

For immunodetection, blots were incubated with primary antibodies overnight at 4 °C and then washed and incubated with horseradish peroxidase (HRP)-conjugated anti-mouse

IgG (H+L) (1:5000, Zhongshan Golden Bridge Biotechnology Co, Ltd, Beijing, China) or HRP-conjugated anti-rabbit IgG (H+L) (1:3000, Zhongshan Golden Bridge Biotechnology Co, Ltd, Beijing, China) for 1 h. ECL Super Signal® West Pico Chemiluminescent Substrate (Pierce) was applied to enable visualization of the bands. The relative levels of each protein to β-actin were determined by densitometry analysis with ImageJ software.

Statistical analysis

All data were expressed as the mean±standard error of the mean (SEM). Groups were compared by one-way analysis of variance (ANOVA), followed by the Student-Newman-Keuls *post hoc* test to detect differences among various groups or two independent-sample *t*-tests to compare differences between two groups. SPSS software (version 18.0) was used for all analyses. *P*-values <0.05 were considered statistically significant.

Results

Quercetin had a protective effect on DRG neuron

MTT reduction assays showed that the cell viability in DRG neurons exposed to HG was significantly reduced compared to that observed in control DRG neurons (Figure 2). Quercetin attenuated HG-induced decreases in cell viability in a dose-dependent manner.

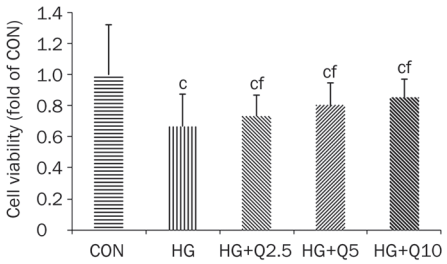

Figure 2. Cell viability data from MTT assays. HG had a negative effect on cell viability, which was expressed as the percentage of cytoprotection compared to the control group (set at 100%) ($^{c}P<0.01$ *vs* CON). Treatment with quercetin resulted in a partial reversal of the HG effect ($^{f}P<0.01$ *vs* HG).

Quercetin inhibited production of HG-induced ROS

The measurement of intracellular hydrogen peroxide levels with the DCFH-DA assay revealed that HG produced a marked increase in intracellular ROS levels, compared to that seen in control cells (Figure 3A, 3B). Quercetin blocked this increase in intracellular ROS in a dose-dependent manner.

Quercetin prevents HG-induced apoptosis of DRG neurons

As shown in Figure 4A–4C, TUNEL analysis showed that the percentages of apoptotic cells were increased in groups exposed to HG. The addition of quercetin reduced the frequency of apoptotic DRG neurons in HG conditions significantly, and these inhibitory effects were dose dependent.

Effects of quercetin on the Nrf-2 and HO-1 expression

After 24 h, Nrf-2 expression was decreased in the HG group, but increased in the HG+quercetin groups, compared with the control group. HO-1 was decreased in the HG group compared with controls. Treatment with quercetin significantly attenuated HG effects on HO-1 protein expression. Indeed, the addition of quercetin normalized levels of Nrf-2 and HO-1 under HG conditions in a dose-dependent manner. Similar patterns of Nrf-2 and HO-1 mRNA transcription were detected across the different groups of cells (Figure 5A–5C).

Effects of quercetin on NF-κB, IκBα, and p-IκBα levels

The induction of inflammatory mediators under HG exposure was paralleled by the upregulation of expression of NF-κB and IκBα, and the phosphorylation of IκBα. Our Western blot experiment revealed that the levels of NF-κB, IκBα, and p-IκBα proteins were higher in cells in the HG condition than those in the control group, which indicated the activation of NF-κB. Compared to HG-exposed cells not treated with quercetin, the

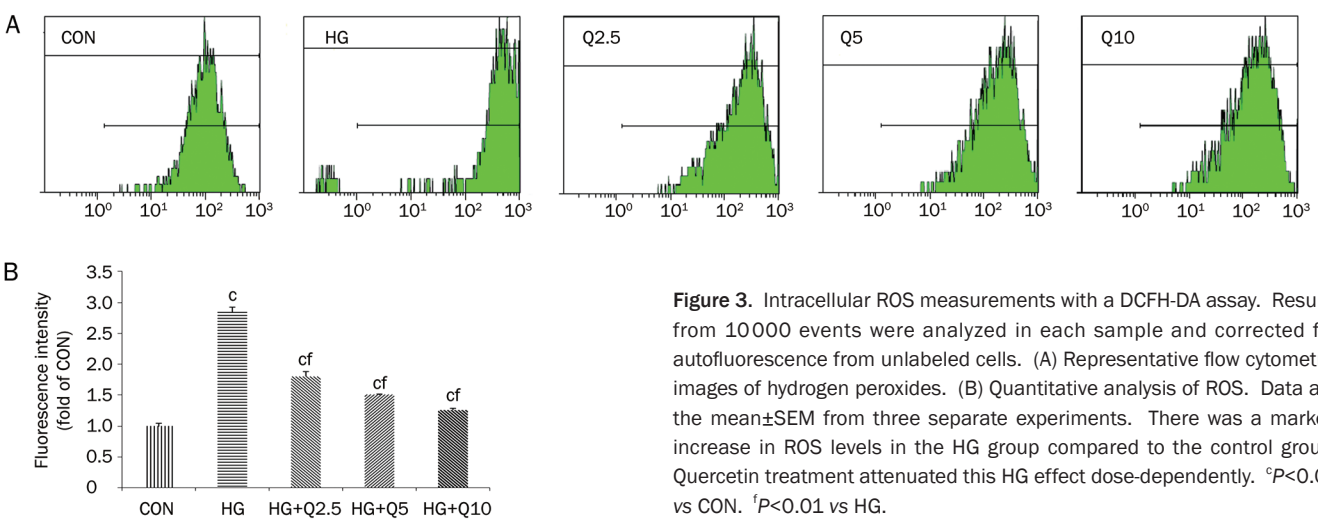

Figure 3. Intracellular ROS measurements with a DCFH-DA assay. Results from 10000 events were analyzed in each sample and corrected for autofluorescence from unlabeled cells. (A) Representative flow cytometric images of hydrogen peroxides. (B) Quantitative analysis of ROS. Data are the mean±SEM from three separate experiments. There was a marked increase in ROS levels in the HG group compared to the control group. Quercetin treatment attenuated this HG effect dose-dependently. $^{c}P<0.01$ *vs* CON. $^{f}P<0.01$ *vs* HG.

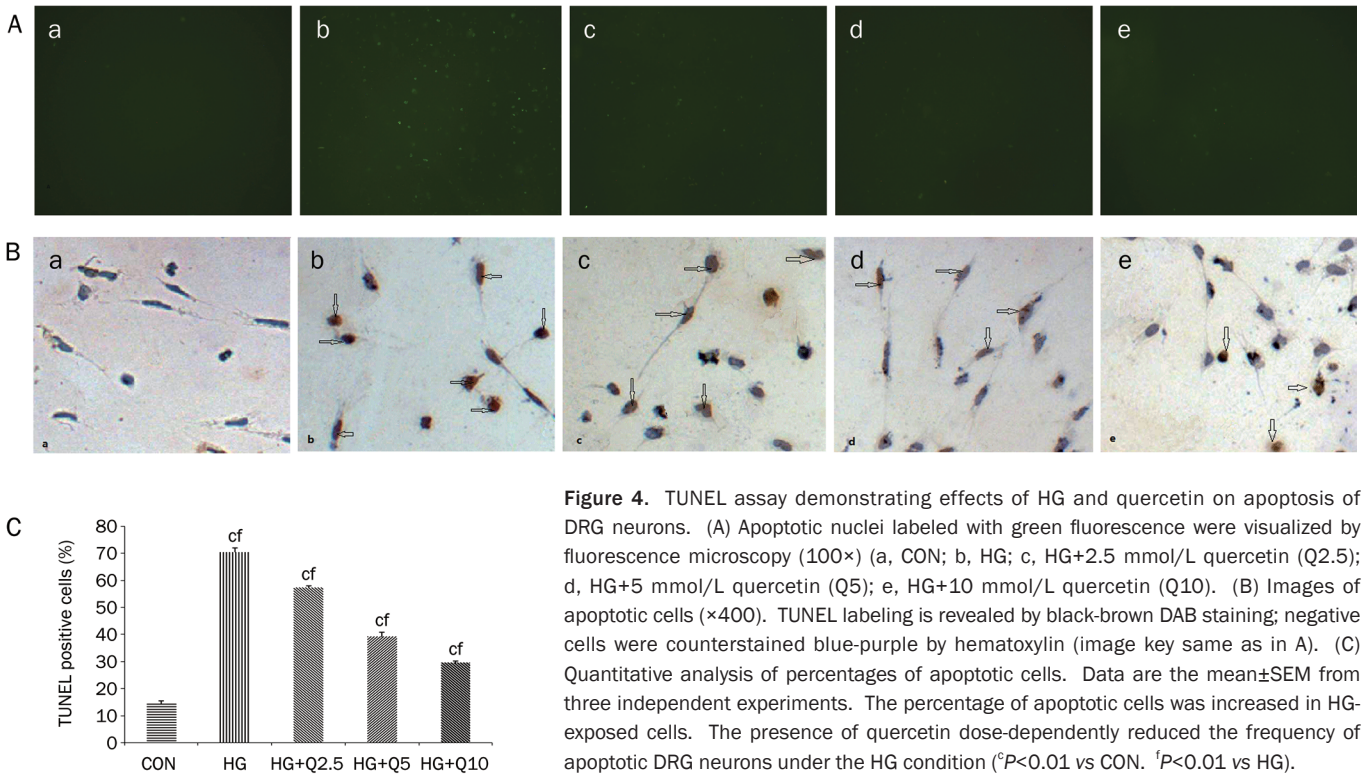

Figure 4. TUNEL assay demonstrating effects of HG and quercetin on apoptosis of DRG neurons. (A) Apoptotic nuclei labeled with green fluorescence were visualized by fluorescence microscopy (100×) (a, CON; b, HG; c, HG+2.5 mmol/L quercetin (Q2.5); d, HG+5 mmol/L quercetin (Q5); e, HG+10 mmol/L quercetin (Q10). (B) Images of apoptotic cells (×400). TUNEL labeling is revealed by black-brown DAB staining; negative cells were counterstained blue-purple by hematoxylin (image key same as in A). (C) Quantitative analysis of percentages of apoptotic cells. Data are the mean±SEM from three independent experiments. The percentage of apoptotic cells was increased in HG-exposed cells. The presence of quercetin dose-dependently reduced the frequency of apoptotic DRG neurons under the HG condition ($^{c}P<0.01$ *vs* CON. $^{f}P<0.01$ *vs* HG).

quercetin-treated and HG-exposed cells had decreased levels of NF-κB, IκBα, and p-IκBα, and these effects were dose-dependent (Figure 6A, 6B). Consistent with these Western blot protein data, our RT-PCR experiment also showed reduced levels of NF-κB mRNA in the quercetin-treated groups (Figure 6C).

Effects of quercetin on IL-6 and TNF-α expression levels

Western blot analysis showed that the IL-6 and TNF-α expression levels, which we employed as biological markers for inflammation, were increased in the HG group compared to the control group. Conversely, these markers were decreased in a dose-dependent manner in the quercetin-treated, HG-exposed cells compared to levels in the nontreated HG-exposed cells (Figure 7A, 7B). Our RT-PCR results indicated that the effects of HG and quercetin on IL-6 and TNF-α mRNA were generally consistent with the Western blot protein data (Figure 7C). However, although we observed significantly higher protein levels of TNF-α and IL-6 in the HG group than in the Q2.5 group, the mRNA transcript levels of these cytokines did not differ significantly between the HG and Q2.5 groups.

Effects of quercetin on iNOS and COX-2 expression

The expression levels of iNOS and COX-2 inducible enzymes that are abundant in cells at sites of inflammation were significantly increased in the HG group compared to the control group. Quercetin treatment reduced the expressions of iNOS and COX-2 in HG-exposed cells. This finding suggests that these enzymes likely mediate the inhibitory influence of quercetin on the activation of the inflammatory cascade. Similar to the above-described observations, the effects of quercetin on the iNOS and COX-2 levels were also dose-dependent (Figure 8A–8C).

Effect of quercetin on caspase-3 activation

Finally, to characterize the hyperglycemia-related apoptosis, relative levels of cleaved and intact caspase-3 were determined by Western blot analysis (Figure 9A, 9B) and real-time PCR (Figure 9C). We found that the inclusion of quercetin in the media significantly reduced the caspase-3 cleavage in a dose-dependent manner, although the levels of intact caspase-3 protein remained stable. Interestingly, caspase-3 mRNA transcription was increased in HG-exposed cells, but to a lesser extent than the change in cleaved caspase-3 protein expression. Treatment of HG-exposed cells with quercetin also produced a downregulation of caspase-3 mRNA transcription relative to the nontreated, HG-exposed cells. Hence, quercetin treatment appeared to counteract the influence of HG exposure on caspase activation in DRG neurons.

Discussion

In this study, we obtained evidence showing that when DRG neurons are exposed to HG, they exhibit decreased cell viability and increased levels of ROS and apoptosis. They also show increased activation of NF-κB and elevated levels of proinflammatory cytokines (IL-6 and TNF-α) and other inflammatory-related enzymes (iNOS and COX-2). Treatment with

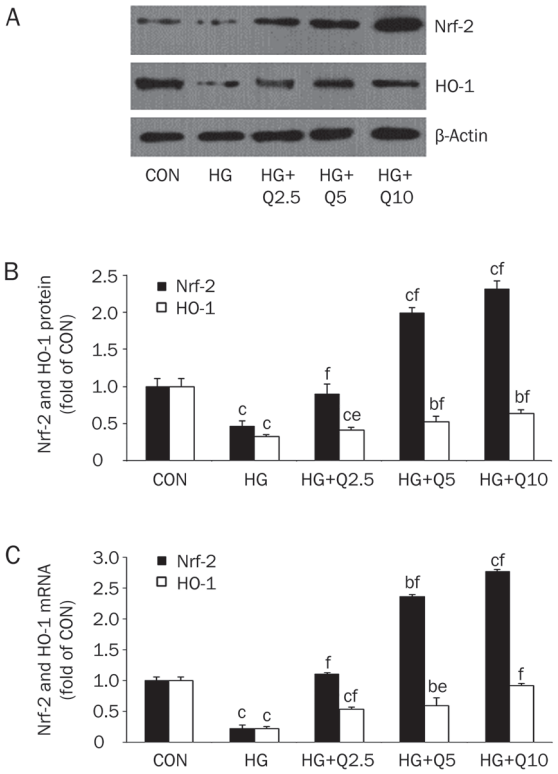

Figure 5. Relative levels of Nrf-2 and HO-1 in different groups of cells as determined by Western blot assays and RT-PCR. (A) Representative Western blots. (B) Quantitative analysis of Nrf-2 and HO-1 protein. Protein expression levels of Nrf-2 and HO-1 were significantly decreased in the HG group compared to the normal glucose exposure control group. Quercetin attenuated the HG-induced reductions in Nrf-2 and HO-1. (C) Relative mRNA transcript levels of Nrf-2 and HO-1. Quercetin normalized the mRNA levels of Nrf-2 and HO-1. Data are the mean±SEM from three independent experiments. $^{b}P<0.05$, $^{c}P<0.01$ *vs* CON. $^{e}P<0.05$, $^{f}P<0.01$ *vs* HG.

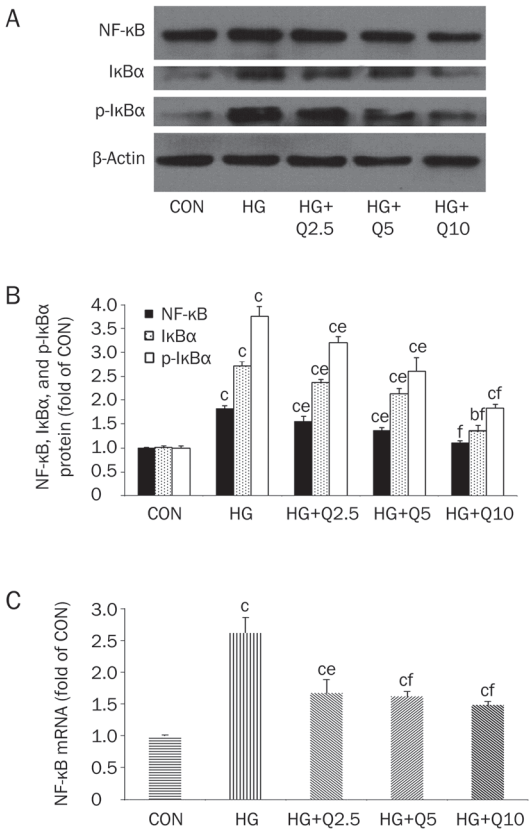

Figure 6. Relative levels of NF-κB, IκBα, and p-IκBα as determined by RT-PCR and Western blot assays. (A) Representative images of Western blots. (B) Quantitative analysis of NF-κB, IκBα, and p-IκBα protein levels. Protein expression levels of NF-κB, IκBα, and p-IκBα were significantly increased in the HG group compared to the normal glucose exposure control group. Quercetin attenuated the effects of HG on the expressions of NF-κB, IκBα, and p-IκBα. (C) Relative mRNA transcript levels of NF-κB. Quercetin normalized the mRNA levels of NF-κB. Data are the mean±SEM from three independent experiments. $^{b}P<0.05$, $^{c}P<0.01$ *vs* CON. $^{e}P<0.05$, $^{f}P<0.01$ *vs* HG.

quercetin attenuated HG-induced apoptosis, and this effect was concomitant with an inhibition of NF-κB, Nrf-2/HO-1, and caspase-3 activity. These effects were associated with the downregulated expressions of IL-6, TNF-α, iNOS, and COX-2. The effects of quercetin on DRG neurons were dose-dependent and detectable at both the protein and mRNA levels.

The present study complements prior research showing decreases in the nuclear localization of NF-κB subunits in HG-exposed DRGs being employed as an *in vitro* analog of peripheral neuropathy. The model is clinically relevant, in that DRGs are nodes of sensory afferent somata, and diabetes-associated numbness and pain in patients can be attributed to dysfunction and apoptosis of DRG neurons[16]. Under these conditions, the changes in NF-κB may be attributable, at least in part, to impaired mitochondrial ROS scavenging due to a deficiency of manganese superoxide dismutase. Importantly, enhancement of NF-κB activity in cultured HG-exposed DRG neurons, similar to that shown here, has been shown by others to ameliorate suboptimal neurite outgrowth[29]. Additionally, Chiarugi[30] demonstrated that drug-dependent inhibition of neuronal NF-κB activity induced selective activation of caspase-9 and -3 and mitochondrial release of cytochrome *c*.

Given their high susceptibility to hyperglycemia, DRG neurons are an attractive target for diabetic neuropathy treatment. In the last decade, researchers have found that DRG neurons in culture died through programmed cell death when exposed to elevated levels of glucose, and confirmed that ROS are an important component of this induction of cell death[17]. Subsequent research revealed additional mechanisms that were contributing to this cell death, including respiratory chain dysfunction, mitochondrial DNA damage, and inflammation[9, 31, 32]. Advanced glycation end products (AGEs) and oxidized lipoproteins activate inflammatory signaling, which leads to oxidative and nitrosative stress, which in turn aggravates the inflammation[4, 33]. Therefore, clearance of oxidative and nitrosative stress and inhibition of inflammation have been considered good strategies for the treatment of diabetic neuropathy[34].

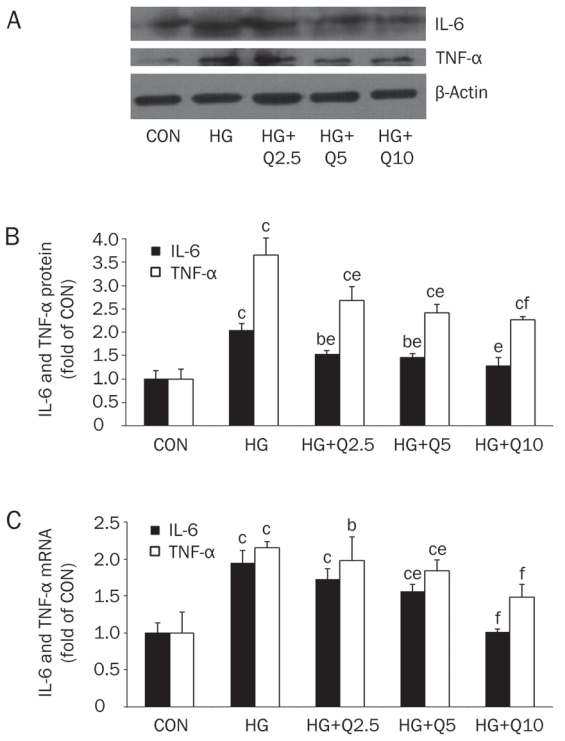

Figure 7. Relative levels of IL-6 and TNF-α expression as determined by Western blot assays and RT-PCR. (A) Representative images of Western blots. (B) Quantitative analysis of IL-6 and TNF-α protein. Protein expression levels of IL-6 and TNF-α were significantly increased in the HG group compared to the control group. Quercetin attenuated the effect of HG on the expressions of IL-6 and TNF-α. (C) Relative mRNA transcript levels of IL-6 and TNF-α. Treatment with quercetin normalized the mRNA levels of IL-6 and TNF-α. Data are the mean±SEM from three independent experiments. $^{b}P<0.05$, $^{c}P<0.01$ *vs* CON. $^{e}P<0.05$, $^{f}P<0.01$ *vs* HG.

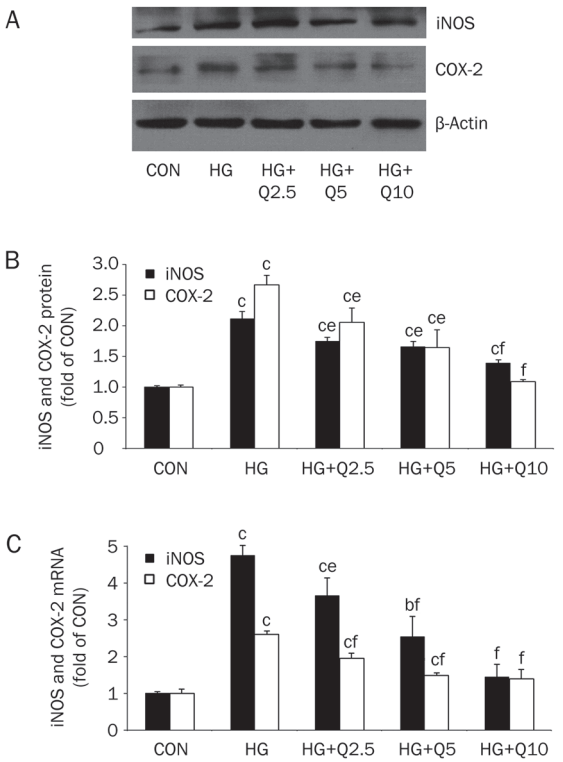

Figure 8. Relative expressions of iNOS and COX-2 as determined by Western blot and RT-PCR experiments. (A) Representative Western blots. (B) Quantitative analysis of iNOS and COX-2 protein. iNOS and COX-2 expression were increased in the HG group compared to the control group. Quercetin attenuated the effects of HG on the expression levels of iNOS and COX-2. (C) Relative mRNA transcript levels of iNOS and COX-2. Quercetin normalized the mRNA levels of iNOS and COX-2. Data are the mean±SEM from three independent experiments. $^{b}P<0.05$, $^{c}P<0.01$ *vs* CON. $^{e}P<0.05$, $^{f}P<0.01$ *vs* HG.

Prior studies have shown that quercetin has a good capacity for scavenging ROS and yielding neuroprotection. Quercetin has been shown to inhibit LPS-induced upregulation of both iNOS and COX-2, as well as expression of p38 mitogen-activated protein kinase (p38-MAPK), TNF-α, and NF-κB[15, 35, 36]. Additionally, quercetin has been reported to reduce DNA fragmentation, the Bax/Bcl-2 ratio, nuclear translocation of apoptosis-inducing factor, and PARP cleavage[37]. Moreover, Arredondo *et al*[38] recently found that quercetin could induce Nrf-2 nuclear translocation and increase the γ-glutamylcysteine ligase catalytic subunit gene expression, and these effects were associated with prevention of neuronal death from oxidant exposure. Thus, the present findings combined with prior findings suggest that quercetin works through multiple pathways to protect neurons from oxidative damage.

Researchers interested in controlling the production of free radicals are particularly interested in antioxidant enzymes, especially superoxide dismutases, catalases, and glutathione peroxidases. Nrf-2 is referred to as the "master regulator" of the antioxidant response because it modulates the expression of hundreds of genes, including not only antioxidant enzymes, but also numerous genes involved in diverse processes such as immune and inflammatory responses[39]. Under quiescent conditions, the repressor of Nrf-2, Kelch-like ECH-associated protein 1 (Keap1), binds Nrf-2 and thereby sequesters it in the cytoplasm. When Keap1 encounters ROS, it dissociates from Nrf-2, leaving Nrf-2 less prone to proteasomal degradation and free to translocate to the nucleus, where it interacts with the antioxidant response element to increase the expression of many antioxidant and detoxifying enzymes and proteins (*eg*, HO-1, NAD(P)H dehydrogenase quinone 1, glutathione S-transferase, and superoxide dismutase). Although brief (<3 h), mild oxidative stress stimulates nuclear transfer of Nrf-2 to produce a protective effect on DRG neurons. Long-term hyperglycemia inhibits the expression of Nrf-2 and depresses the expression of HO-1[9, 40]. Our findings suggest that quercetin alleviates the negative long-term effects of HG by upregulating the expressions of Nrf-2 and HO-1.

NF-κB can be activated by many factors, including, in addition to hyperglycemia, hypoxia, ischemia, and infection. Exposure to HG can affect NF-κB expression through various pathways, with hyperglycemia-related ROS being a major factor[41, 42]. Hyperglycemia can trigger phosphatidyl inositide-

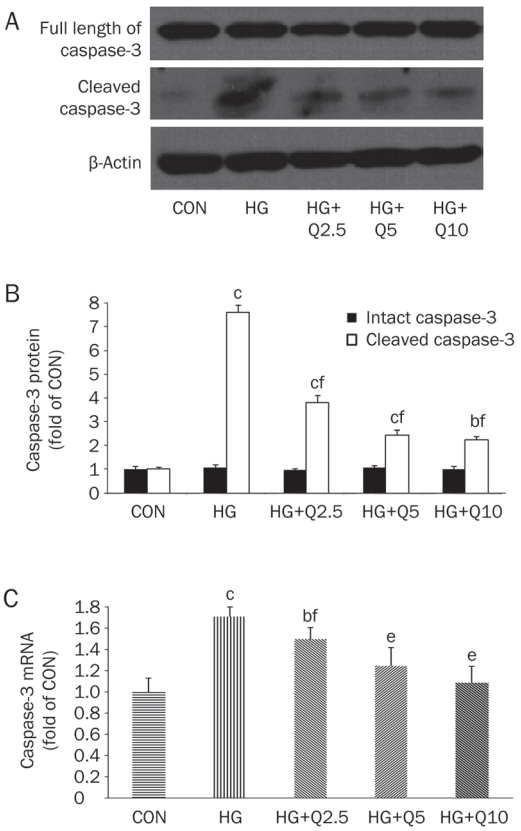

Figure 9. Caspase-3 levels as determined Western blot assays and RT-PCR. (A) Representative images. (B) Quantitative analysis of the cleaved caspase-3. Relative levels of cleaved caspase-3 were increased markedly in HG-treated cells compared to normal glucose conditions. Addition of quercetin reduced caspase-3 cleavage induced by HG in a dose-dependent manner. Intact caspase-3 levels were similar across all five groups. (C) Relative mRNA transcript levels of caspase-3. Quercetin normalized the mRNA levels of caspase-3, but not in parallel with caspase-3 protein, which indicates that quercetin decreases the apoptosis of DRG neurons mainly by inhibiting the cleavage of caspase-3. Quantitative data are expressed as the mean±SEM from three independent experiments. $^{b}P<0.05$, $^{c}P<0.01$ *vs* CON. $^{e}P<0.05$, $^{f}P<0.01$ *vs* HG.

3-kinase/Akt signaling and induce NF-κB-related upregulation of COX-2, which in turn triggers proapoptotic caspase-3 activity[43]. Other researchers have found that NADPH oxidase-related ROS-induced apoptosis is mediated via JNK-dependent activation of NF-κB in cardiomyocytes exposed to HG[44]. Additionally, AGE-induced ROS generation also triggers NF-κB activation and subsequent TNF-α production to induce apoptosis[45]. Treatment with an NF-κB inhibitor has been reported to prevent AGE-induced iNOS expression by interfering with p38 MAPK activity[46].

In conclusion, the present experiments demonstrated that apoptosis of DRG neurons was increased under HG (diabetes model) conditions, and this effect was attenuated in the presence of quercetin. Our data further suggest that these protective effects of quercetin may be attributable to influences on the Nrf-2/HO-1 pathway, scavenging ROS, and inhibition of NF-κB activation. The possibility that NF-κB may play a critical role in the pathogenesis of neuronal dysfunction due to hyperglycemia suggests that the inhibition of local NF-κB activity may be a beneficial strategy for preventing or alleviating diabetic neuropathy complications. Furthermore, our findings of the protective effects of quercetin on DRG neurons in a hyperglycemic environment point to quercetin as a potential medicine for diabetic neuropathy.

Acknowledgements

The authors would like to thank the Department of TCM at PUMCH and the Institute of Basic Medical Sciences of Chinese Academy of Medical Sciences, Beijing, China for supporting this research. We thank Medjaden Bioscience Limited for assisting in the preparation of this manuscript.

Author contribution

Yue SHI, Xiao-chun LIANG, and Hong ZHANG designed the research; Yue SHI and Hong ZHANG performed the research; Qun-li WU, Ling QU, and Qing SUN contributed new reagents and analytic tools; Yue SHI analyzed the data; and Yue SHI wrote the paper.

References

1 Smith AG, Singleton JR. Diabetic neuropathy. Continuum (Minneap Minn) 2012; 18: 60–84.
2 Sumner CJ, Sheth S, Griffin JW, Cornblath DR, Polydefkis M. The spectrum of neuropathy in diabetes and impaired glucose tolerance. Neurology 2003; 60: 108–11.
3 Singleton JR, Smith AG, Bromberg MB. Increased prevalence of impaired glucose tolerance in patients with painful sensory neuropathy. Diabetes Care 2001; 24: 1448–53.
4 Vincent AM, Callaghan BC, Smith AL, Feldman EL. Diabetic neuropathy: cellular mechanisms as therapeutic targets. Nat Rev Neurol 2011; 7: 573–83.
5 Edwards JL, Vincent AM, Cheng HT, Feldman EL. Diabetic neuropathy: mechanisms to management. Pharmacol Ther 2008; 120: 1–34.
6 Vincent AM, Edwards JL, Sadidi M, Feldman EL. The antioxidant response as a drug target in diabetic neuropathy. Curr Drug Targets 2008; 9: 94–100.
7 Sheetz MJ, King GL. Molecular understanding of hyperglycemia's adverse effects for diabetic complications. JAMA 2002; 288: 2579–88.
8 Negi G, Kumar A, Joshi RP, Sharma SS. Oxidative stress and Nrf2 in the pathophysiology of diabetic neuropathy: old perspective with a new angle. Biochem Biophys Res Commun 2011; 408: 1–5.
9 Negi G, Kumar A, Sharma SS. Melatonin modulates neuroinflammation and oxidative stress in experimental diabetic neuropathy: effects on NF-kappaB and Nrf2 cascades. J Pineal Res 2011; 50: 124–31.
10 Kumar A, Sharma SS. NF-kappaB inhibitory action of resveratrol: a probable mechanism of neuroprotection in experimental diabetic neuropathy. Biochem Biophys Res Commun 2010; 394: 360–5.
11 Kumar A, Negi G, Sharma SS. Suppression of NF-kappaB and NF-kappaB regulated oxidative stress and neuroinflammation by BAY 11-7082 (IkappaB phosphorylation inhibitor) in experimental diabetic neuropathy. Biochimie 2012; 94: 1158–65.
12 Hovaguimian A, Gibbons CH. Clinical Approach to the Treatment of Painful Diabetic Neuropathy. Ther Adv Endocrinol Metab 2011; 2: 27–38.

13 Firuzi O, Miri R, Tavakkoli M, Saso L. Antioxidant therapy: current status and future prospects. Curr Med Chem 2011; 18: 3871–88.
14 Boots AW, Haenen GR, Bast A. Health effects of quercetin: from antioxidant to nutraceutical. Eur J Pharmacol 2008; 585: 325–37.
15 Zhang ZJ, Cheang LC, Wang MW, Lee SM. Quercetin exerts a neuroprotective effect through inhibition of the iNOS/NO system and pro-inflammation gene expression in PC12 cells and in zebrafish. Int J Mol Med 2011; 27: 195–203.
16 McHugh JM, McHugh WB. Diabetes and peripheral sensory neurons: what we don't know and how it can hurt us. AACN Clin Issues 2004; 15: 136–49.
17 Vincent AM, McLean LL, Backus C, Feldman EL. Short-term hyperglycemia produces oxidative damage and apoptosis in neurons. FASEB J 2005; 19: 638–40.
18 Yamakawa I, Kojima H, Terashima T, Katagi M, Oi J, Urabe H, *et al*. Inactivation of TNF-alpha ameliorates diabetic neuropathy in mice. Am J Physiol Endocrinol Metab 2011; 301: E844–E852.
19 Ma W, Chabot JG, Vercauteren F, Quirion R. Injured nerve-derived COX2/PGE2 contributes to the maintenance of neuropathic pain in aged rats. Neurobiol Aging 2010; 31: 1227–37.
20 Russell JW, Sullivan KA, Windebank AJ, Herrmann DN, Feldman EL. Neurons undergo apoptosis in animal and cell culture models of diabetes. Neurobiol Dis 1999; 6: 347–63.
21 Rubiolo JA, Mithieux G, Vega FV. Resveratrol protects primary rat hepatocytes against oxidative stress damage: activation of the Nrf2 transcription factor and augmented activities of antioxidant enzymes. Eur J Pharmacol 2008; 591: 66–72.
22 Yang L, Shen J, He S, Hu G, Shen J, Wang F, *et al*. L-cysteine administration attenuates pancreatic fibrosis induced by TNBS in rats by inhibiting the activation of pancreatic stellate cell. PLoS One 2012; 7: e31807.
23 Ndisang JF, Lane N, Syed N, Jadhav A. Up-regulating the heme oxygenase system with hemin improves insulin sensitivity and glucose metabolism in adult spontaneously hypertensive rats. Endocrinology 2010; 151: 549–60.
24 Puxeddu E, Knauf JA, Sartor MA, Mitsutake N, Smith EP, Medvedovic M, *et al*. RET/PTC-induced gene expression in thyroid PCCL3 cells reveals early activation of genes involved in regulation of the immune response. Endocr Relat Cancer 2005; 12: 319–34.
25 López-Posadas R, Requena P, González R, Suárez MD, Zarzuelo A, Sánchez de Medina F, *et al*. Bovine glycomacropeptide has intestinal antiinflammatory effects in rats with dextran sulfate-induced colitis. J Nutr 2010; 140: 2014–49.
26 Zhang C, Lei GS, Shao S, Jung HW, Durant PJ, Lee CH. Accumulation of myeloid-derived suppressor cells in the lungs during Pneumocystis pneumonia. Infect Immun 2012; 80: 3634–41.
27 Neeb L, Hellen P, Boehnke C, Hoffmann J, Schuh-Hofer S, Dirnagl U, *et al*. IL-1beta stimulates COX-2 dependent PGE(2) synthesis and CGRP release in rat trigeminal ganglia cells. PLoS One 2011; 6: e17360.
28 Hellmich HL, Eidson K, Cowart J, Crookshanks J, Boone DK, Shah S, *et al*. Chelation of neurotoxic zinc levels does not improve neurobehavioral outcome after traumatic brain injury. Neurosci Lett 2008; 440: 155–9.
29 Saleh A, Schapansky J, Smith DR, Young N, Odero GL, Aulston B, *et al*. Normalization of NF-kappaB activity in dorsal root ganglia neurons cultured from diabetic rats reverses neuropathy-linked markers of cellular pathology. Exp Neurol 2013; 241: 169–78.
30 Chiarugi A. Characterization of the molecular events following impairment of NF-kappaB-driven transcription in neurons. Brain Res Mol Brain Res 2002; 109: 179–88.
31 Akude E, Zherebitskaya E, Chowdhury SK, Smith DR, Dobrowsky RT, Fernyhough P. Diminished superoxide generation is associated with respiratory chain dysfunction and changes in the mitochondrial proteome of sensory neurons from diabetic rats. Diabetes 2011; 60: 288–97.
32 Lupachyk S, Shevalye H, Maksimchyk Y, Drel VR, Obrosova IG. PARP inhibition alleviates diabetes-induced systemic oxidative stress and neural tissue 4-hydroxynonenal adduct accumulation: correlation with peripheral nerve function. Free Radic Biol Med 2011; 50: 1400–9.
33 Vincent AM, Perrone L, Sullivan KA, Backus C, Sastry AM, Lastoskie C, *et al*. Receptor for advanced glycation end products activation injures primary sensory neurons via oxidative stress. Endocrinology 2007; 148: 548–58.
34 Tahrani AA, Askwith T, Stevens MJ. Emerging drugs for diabetic neuropathy. Expert Opin Emerg Drugs 2010; 15: 661–83.
35 Cho N, Choi JH, Yang H, Jeong EJ, Lee KY, Kim YC, *et al*. Neuroprotective and anti-inflammatory effects of flavonoids isolated from *Rhus verniciflua* in neuronal HT22 and microglial BV2 cell lines. Food Chem Toxicol 2012; 50: 1940–5.
36 Dai X, Ding Y, Zhang Z, Cai X, Li Y. Quercetin and quercitrin protect against cytokineinduced injuries in RINm5F beta-cells via the mitochondrial pathway and NF-kappaB signaling. Int J Mol Med 2013; 31: 265–71.
37 Bournival J, Francoeur MA, Renaud J, Martinoli MG. Quercetin and sesamin protect neuronal PC12 cells from high-glucose-induced oxidation, nitrosative stress, and apoptosis. Rejuvenation Res 2012; 15: 322–33.
38 Arredondo F, Echeverry C, Abin-Carriquiry JA, Blasina F, Antúnez K, Jones DP, *et al*. After cellular internalization, quercetin causes Nrf2 nuclear translocation, increases glutathione levels, and prevents neuronal death against an oxidative insult. Free Radic Biol Med 2010; 49: 738–47.
39 Hybertson BM, Gao B, Bose SK, McCord JM. Oxidative stress in health and disease: the therapeutic potential of Nrf2 activation. Mol Aspects Med 2011; 32: 234–46.
40 Vincent AM, Kato K, McLean LL, Soules ME, Feldman EL. Sensory neurons and schwann cells respond to oxidative stress by increasing antioxidant defense mechanisms. Antioxid Redox Signal 2009; 11: 425–38.
41 Nambu H, Kubo E, Takamura Y, Tsuzuki S, Tamura M, Akagi Y. Attenuation of aldose reductase gene suppresses high-glucose-induced apoptosis and oxidative stress in rat lens epithelial cells. Diabetes Res Clin Pract 2008; 82: 18–24.
42 Busik JV, Mohr S, Grant MB. Hyperglycemia-induced reactive oxygen species toxicity to endothelial cells is dependent on paracrine mediators. Diabetes 2008; 57: 1952–65.
43 Sheu ML, Ho FM, Yang RS, Chao KF, Lin WW, Lin-Shiau SY, *et al*. High glucose induces human endothelial cell apoptosis through a phosphoinositide 3-kinase-regulated cyclooxygenase-2 pathway. Arterioscler Thromb Vasc Biol 2005; 25: 539–45.
44 Kuo WW, Wang WJ, Tsai CY, Way CL, Hsu HH, Chen LM. Diallyl trisufide (DATS) suppresses high glucose-induced cardiomyocyte apoptosis by inhibiting JNK/NFkappaB signaling via attenuating ROS generation. Int J Cardiol 2012; doi: 10.1016/j.ijcard.2012.09.080.
45 Morita M, Yano S, Yamaguchi T, Sugimoto T. Advanced glycation end products-induced reactive oxygen species generation is partly through NF-kappa B activation in human aortic endothelial cells. J Diabetes Complications 2013; 27: 11–5.
46 Chang PC, Chen TH, Chang CJ, Hou CC, Chan P, Lee HM. Advanced glycosylation end products induce inducible nitric oxide synthase (iNOS) expression via a p38 MAPK-dependent pathway. Kidney Int 2004; 65: 1664–75.